An Evaluation of Analog and Numerical Techniques for Unsteady Heat Transfer Measurement with Thin Film Gauges in Transient Facilities

William K. George*, William J. Rae* and Scott H. Woodward**
Calspan-UB Research Center
Buffalo, NY 14260

ABSTRACT

The importance of frequency response considerations in the use of thin film gauges for unsteady heat transfer measurements in transient facilities has been considered and methods for evaluating it have been proposed. A departure frequency response function has been introduced and illustrated by an existing analog circuit. A Fresnel integral temperature which possesses the essential features of the film temperature in transient facilities has been introduced and used to evaluate two numerical algorithms. Finally criteria have been proposed for the use of finite difference algorithms for the calculation of the unsteady heat flux from a sampled temperature signal.

---

*Professor of Mechanical & Aerospace Engineering, University at Buffalo, SUNY
**Research Scientist, Turbulence Research Laboratory, University at Buffalo, SUNY

INTRODUCTION

The use of thin film gauges for heat transfer measurement in transient facilities has been well-established over the past 30 years (Vidal, [1]; see Schultz and Jones [2] for an excellent review). Until recently, attention was focused on either relatively simple flows (such as the passage of a shock wave) or on attempts to measure "mean" heat transfer rates on gas turbine blades under quasi-steady conditions. In both types of experiments, attention was focused on capturing the rise in temperature and mean heat flux, and the fluctuations due to periodic flow disturbances or turbulence were of little interest. In recent years there has been considerable interest in extending the thin film technique to the measurement of fluctuating heat transfer rates in transient experiments, especially with regard to gas turbine applications (Dunn and Holt,[3]; Dunn et al. [4], [5] and Doorly, [6]). All of these experiments used an analog circuit, hereafter referred to as the Q-meter, to convert the surface temperature measured by the thin film gauges to heat flux signals. The Q-meter was originally developed in the late 1950's (Skinner [7], Meyer [8]), and was redesigned by Oldfield et al. [9] to the wide band analog used in this report. While this circuit has the advantage of directly presenting an analog voltage proportional to heat transfer rate, its design is based on the assumption of constant thermal properties of the substrate, a condition violated in some experiments. Moreover, the Q-meter, although a considerable improvement over the original designs, has a bandwidth substantially lower than that of the gauge itself.

An alternative to the Q-meter is to directly record the surface temperatures, and then calculate the heat flux numerically from either the one-dimensional heat transfer equation or an analytic solution to it. One of the most successful examples of the latter is the numerical algorithm of Cook and Felderman [10] and Cook [11] which assumed constant thermal properties.

and

$$\angle \hat{q}(0,f) = \angle \hat{T}(0,f) + 45^{o} \tag{5}$$

AMPLITUDE AND PHASE RESPONSE

The ideal analog Q-meter would be one which duplicates the response characteristics of equations (3)-(5) over the frequency range of interest. Any deviation from this ideal characteristic will result in a distortion of the unsteady heat transfer signal.

That this is indeed the case can be seen by viewing the Q-meter as a linear circuit as shown in Figure 2a. For such systems the Fourier transform of the output is simply the Fourier transform of the input multiplied by the frequency response function of the system.* Thus if $\hat{e}_i(f)$ and $\hat{e}_{oi}(f)$ represent the input and output to this ideal system,

$$\hat{e}_{oi}(f) = H_{ideal}(f)\ \hat{e}_i(f) \tag{6}$$

The ideal frequency response function for a Q-meter would be (to within a factor dependent on the thermal properties of the substrate)

$$H_{ideal}(f) = \sqrt{j2\pi f} \tag{7}$$

In practice, circuits are never ideal. These departures can often be characterized by introducing a hypothetical filter as shown in Figure 2b which accounts for the departures from the ideal. The output from the real system can be written as

$$\begin{aligned} \hat{e}_o(f) &= H_{dep}(f)\ \hat{e}_{oi} \\ &= H_{dep}(f)\ H_{ideal}(f)\ \hat{e}_i(f) \end{aligned} \tag{8}$$

The product $H_{dep}(f)\ H_{ideal}(f)$ is thus the real response of the analog, $H_{real}(f)$. Thus the frequency response function of the departure from ideal

---

* The frequency response function of a system is the Fourier transform of the impulse response function of that system.

cross-spectral information if the phase characteristics of all Q-meters is not the same.

Figures 5 and 6 show the effect of the departures from ideal on two typical heat flux signals. Figure 5 shows the response of the analog to a square wave with a fundamental frequency of 13 kHz. Figure 6 shows the response of the analog to a pulse train with fundamental frequency also chosen at 13 kHz and pulse width equal to 1/7 of the period. Unlike the square wave response which is reasonable, the pulse train shows considerable distortion because of the removal of the harmonics by the finite bandwidth of the analog. Without some careful thought about the representative Fourier series for the pulse train, it might have been very difficult to have guessed the real wave form from the analog output, especially in view of the negative regions of the signal. Thus the importance of knowing the frequency response of the system cannot be underestimated if the original waveform is to be determined.

A MODEL FOR THE UNSTEADY TEMPERATURE SIGNAL

The unsteady temperature signal from a thin film gauge on the rotor of a turbine blade in a transient test facility (in this case a shock tunnel) is shown in Figure (7). The rapid rise in temperature is associated with the arrival of the test gas and marks a step change in the heat flux. The temperature signal rises with an approximately $t^{1/2}$. dependence because of the heat transfer to the substrate. Superimposed on the overall rise are the fluctuations resulting from the vane-wake crossings and other unsteady effects in the flow.

One of the difficulties in testing either analog circuits or numerical algorithms is the difficulty in generating a known temperature input signal which possesses the characteristics of a transient experiment like that described above. A particularly useful choice for a test signal would be one

can be determined as:

$$H_{dep}(f) = H_{real}(f)/H_{ideal}(f) \quad (9)$$

Since, in general, the frequency response function is complex, the departures from ideal can be in both the amplitude and phase.

The effect of attenuating the higher Fourier components by a roll-off in the amplitude response is generally well understood. The effect of phase errors can be much more difficult to assess since, in effect, some Fourier components are delayed with respect to others so that the wave forms are distorted. An important exception occurs when the phase errors vary linearly with frequency in which case all Fourier components are delayed by a fixed time delay and no distortion occurs.

Figures 3a and 3b show the amplitude and phase characteristics* of the Q-meter design due to Oldfield et al. [9]. As shown in the preceding section, it is the departure frequency response function which is primarily of interest here. Figures 4a and 4b plot the amplitude and phase characteristics of the departure. The linear-linear plot of the amplitude in Figure (4a) makes it clear that there is considerable attenuation at frequencies well below the half-power points, a fact often obscured by the usual log-log plots. It is also clear from both Figures 3b and 4b that the Q-meter does not produce the desired 45^{o} phase shift. Fortunately, however, the phase shift is linear with frequency below the half-power point (~100 kHz). As pointed out earlier, this means that the individual Fourier components are not shifted with respect to each other, but that the entire signal is delayed by an amount $A/2\pi$ where A is the constant of proportionality between the phase shift Δ and the frequency f. The lag for the circuit shown is ~4 μs. Note that even this linear phase shift can pose a problem when more than one gauge is to be used to obtain

*The authors are grateful to Dr. Martin Oldfield of Oxford University and Dr. James O'Brien of NASA/Lewis for providing the data for Figures 3 and 4.

Dunn et al. [5] attempted to include variable thermal properties by numerically solving the governing equations using the thin film surface temperature data as input. Prior to the present work, a portion of which was reported by Dunn et al. [5], there appears to have been no attempt to analyze the ability of these numerical techniques to resolve fluctuating heat transfer rates.

The purpose of this paper is to present a detailed evaluation of the frequency response of both analog and numerical approaches to the determination of fluctuating heat transfer rates from the output of thin film gauges in transient environments. The amplitude and phase errors are determined and their effect on simulated signals is assessed.

THE PRINCIPLE AND GOVERNING EQUATIONS

Transient heat transfer measurements with thin film gauges depend primarily on the applicability of one-dimensional heat conduction as shown in Figure 1 so that the process can be described by the one-dimensional equation

$$\rho C \frac{\partial T}{\partial t} = \frac{\partial}{\partial x}\left[k \frac{\partial T}{\partial x}\right] \tag{1}$$

subject to the surface condition

$$\dot{q}(0,T) = -k \left.\frac{\partial T}{\partial x}\right|_{x=0} \tag{2}$$

For constant thermal properties, this equation can be solved analytically using Laplace or Fourier transform techniques. If $\hat{T}(0,f)$ and $\hat{q}(0,f)$ are the Fourier transforms of the surface temperature and heat flux, respectively, then

$$\hat{q}(0,f) = \sqrt{\rho Ck}\,\sqrt{j2\pi f}\,\hat{T}(0,f) \tag{3}$$

from which it follows that the modulii and phases are related by

$$|\hat{q}(0,f)| = \sqrt{\rho Ck}\,\sqrt{2\pi f}\;\;|\hat{T}(0,f)| \tag{4}$$

which yields a step change in heat flux (corresponding to the test initiation in a transient facility) superimposed on which is a sinusiodally oscillating unsteady heat flux. Such a heat flux signal is given by

$$q(0,t) = A_0 + A_1 \cos 2\pi f_0 t + B_1 \sin 2\pi f_0 t \tag{10}$$

where f_0 is a given frequency, and where A_0, A_1 and B_1 are arbitrarily chosen coefficients. This is shown in figure (8a), and corresponds to a single Fourier component plus the dc part of the signal which might be seen in a transient facility. If the temperature signal which produces such a heat flux could be determined, it could be utilized to test numerical algorithms designed to directly calculate the heat flux from the measured surface temperature.

For constant thermal properties and zero film thickness, equations (1) and (2) can be solved analytically to yield (Vidal, [1]),

$$T(0,t) = \frac{1}{\sqrt{\pi \rho C k}} \int_0^t \frac{\dot{q}(0,\lambda)}{\sqrt{t-\lambda}}\, d\lambda + T_0 \tag{11}$$

Substitution of equation (10) into equation (11) yields after integration,

$$\sqrt{2\pi f_0}\ \frac{\sqrt{\pi \rho C k}}{A_0}\, T(0,t) = \sqrt{8\pi f_0 t} +$$

$$\sqrt{2\pi} \left\{ C(2\pi f_0 t) \left[\frac{A_1}{A_0} \cos 2\pi f_0 t + \frac{B_1}{A_0} \sin 2\pi f_0 t \right] \right.$$

$$\left. + S(2\pi f_0 t) \left[\frac{A_1}{A_0} \sin 2\pi f_0 t + \frac{B_1}{A_0} \cos 2\pi f_0 t \right] \right\} \tag{12}$$

where

$$C(u) = \frac{1}{\sqrt{2\pi}} \int_0^u \frac{\cos\alpha}{\sqrt{\alpha}}\, d\alpha \tag{13}$$

and

$$S(u) = \frac{1}{\sqrt{2\pi}} \int_0^u \frac{\sin\alpha}{\sqrt{\alpha}}\, d\alpha \tag{14}$$

The integrals C(u) and S(u) can be recognized as the familiar Fresnel integrals, Abramowitz and Stegun [12]. Figure (8b) shows the temperature variation which would produce the heat transfer signal corresponding to $A_1 = 0$, $B_1/A_0 = 1/4$. Because the Fresnel integrals in equation (12) can be evaluated by a variety of convenient formulae, the temperature history of equation (12) is particularly useful for testing finite difference algorithms for solving equation (1) with unsteady inputs. It can also be used to evaluate the overall phase and amplitude response of the data processing system if the impulse response function of the system is known.

Before using the Fresnel-integral temperature history, it is interesting to look at the asymptotic behavior of equation (12). It is straightforward to show by using the asymptotic expansions of the integrals C and S (Abramowitz and Stegun, [12]) that for $2\pi f_0 t \gg 1$,

$$\sqrt{2\pi f_0}\,\frac{\sqrt{\pi\rho Ck}}{A_0}\,T(0,t) = \sqrt{8\pi f_0 t}\left\{1 + \frac{\sqrt{2\pi}}{\sqrt{8\pi f_0 t}}\left[\frac{1}{2} + \frac{\gamma \sin 2\pi f_0 t}{\sqrt{2\pi f_0 t}} + \ldots\right]\left[\frac{A_1}{A_0}\cos 2\pi f_0 t + \frac{B_1}{A_0}\sin 2\pi f_0 t\right] + \left[\frac{1}{2} - \frac{\gamma \cos 2\pi f_0 t}{\sqrt{2\pi f_0 t}} + \ldots\right]\left[\frac{A_1}{A_0}\sin 2\pi f_0 t - \frac{B_1}{A_0}\cos 2\pi f_0 t\right]\right\} \qquad (15)$$

The neglected terms are of order $(2\pi f_0 t)^{-1}$ and the expansion is valid for $2\pi f_0 t > 40$ (or after about six cycles).

The $t^{1/2}$ dependence can be recognized as the surface temperature rise due to a step change in heat flux applied to a semi-infinite slab. Of particular interest to the experimentalist is the fact that the ratio of the fluctuating part of the temperature to the $t^{1/2}$ rise is continuously reduced with time. This makes it very difficult to directly sample the film temperature signal without burying the fluctuating part in the quantization noise of the A/D

Implicit numerical procedures for solving equation (15) work best when the step-size ratio

$$r = \alpha\Delta t/(\Delta x)^2 \qquad (21)$$

is in the range 0.25 to 0.5 [16]. It happens that this criterion can be met for the test conditions of interest here by taking the sampling interval, Δt, on the basis of the Nyquist criterion to be inversely proportional to the highest frequency of interest, i.e. $\Delta t \sim \pi/\omega \sim 1/2f$. The spatial step size Δx must be small enough to resolve the skin depth; that is, $\Delta x \leq \sqrt{\alpha/\omega}$. A constant value of the step-size ratio r will satisfy both of these criteria.

EVALUATION OF NUMERICAL ALGORITHM

The purpose of this section is to evaluate the algorithms outlined above by using the Fresnel integral temperature proposed earlier. Of special concern to the experimentalist is the rate at which data must be taken relative to the frequencies of interest, and the sensitivity of the algorithms to noise on the sampled signal or introduced by the sampling process.

Digital temperature data were generated using the Fresnel integral temperature given by equation 12 and shown in Figure 8b. These data were sampled at rates of 3.75, 7.5, 15 and 30 times the fundamental, and then used as input to the numerical algorithms.

Figures 9 – 12 demonstrate the relative abilities of the Cooke-Felderman algorithm of equation (17) and the simple implicit scheme of equation (19). Note that the progressively poorer reconstruction of the sine wave part of the signal with decreasing number of points for cycle is due to the fact that the graphs have been produced using straight line segments, a procedure generally requiring about 10 points per cycle to produce a smooth sinusoidal. Of more concern here are the magnitude and phase errors of the computed heat flux signals relative to the exact signals. It is clear from the figures that both algorithms suffer from a slight phase lag (about 20 deg.) for the lowest

SUMMARY AND CONCLUSIONS

The use of thin film gauges for the measurement of unsteady heat transfer in transient facilities has been briefly reviewed, with particular attention to how the heat transfer is determined from the film temperature. The removal of Fourier components by the finite frequency response of analog Q-meters was shown to have a significant effect on the heat transfer inferred. Similarly, the sampling rate and choice of computational algorithm was shown to introduce similar problems for the numerical reconstruction of the unsteady heat transfer from the digitally sampled film temperature. The digital methods have the advantage that they require less hardware, and can easily include the effects of the temperature dependent thermal properties of the substrate.

The fundamental frequency limitations of thin film gauges have not been discussed, but will be mentioned briefly here. The upper frequency limit is proportional to $(\alpha_f/d^2)^{1/2}$ where α_f is the thermal diffusivity of the film itself and d is its thickness, v. reference [2]. This is typically of order 10^6 Hz, and is therefore well above the bandwidth of most applications. The principal determinant of the lowest frequency which can be measured is the penetration depth which must be small compared to the size of the film so that the heat transfer into the substrate is effectively one-dimensional. Thus, if ℓ is the smaller of the gauge dimension and the depth of the substrate, the lower cut-off frequency is of order $(\alpha/\ell^2)^{1/2}$ where α is the thermal diffusivity of the substrate, v. reference [2]. Analog Q-meters can deviate from the $f^{1/2}$ response at substantially higher frequencies because of design limitations. It is easy to see that these lower frequency limits place an upper limit on the duration of the test in transient facilities -- at least for which the determination of heat flux from the methods discussed here will be valid.

Finally, it should be noted that there are situations where thin film

sampling rate (Figure 12). This has virtually disappeared for the Cooke-Felderman algorithm when the sampling rate has increased to f_s/f_o = 15 (Figure 10), but persists to even f_s/f_o = 30 (Figure 9) for the simple implicit algorithm. Figure 13 shows how the relative magnitudes of the sinusoidal part of the signal vary with the sampling rate. The Cooke-Felderman algorithm slightly over-predicts the peaks while the simple implicit under-predicts them. Both algorithms converge toward the correct amplitude as the sampling rate increases.

In order to assess the sensitivity to noise on the input data, a second set of input data was generated by truncating the digital word size of the input data to a single byte. The effect is to introduce a quantization noise on the signal which is the same as if it had been sampled by an 8 bit A/D converter. (Note this is a relatively large amount of noise since most A/D converters that would be employed for unsteady signal measurement are 10 bits or greater.) Figure 14a shows a typical quantized input signal while Figure 14b shows the difference between quantized and original input signal. The "noise level" is most easily characterized by defining ϵ to be the ratio of the size of the quantized step to the peak-to-peak fluctuating part of the temperature. For the case shown here and in the subsequent applications, $\epsilon \approx 0.012$.

Figures 15a-d show the effect of the 8-bit quantization on the Cooke-Felderman algorithm for the four sampling rates. These can be compared to the simple implicit results shown in Figures 16a-d. Both algorithms show a slight increase in the noise present on the signal with increasing sampling rate. The simple implicit algorithm, however, is less sensitive to noise than is the Cooke-Felderman. This can probably be attributed to its poorer frequency response which effectively low-pass filters the quantization noise.

converter. The Q-meter with its $\sqrt{f}$ response tends to alleviate this problem as does the differentiation approach of Dunn et al. [5].

In the following section the Fresnel integral temperature history will be used to evaluate several numerical schemes for directly evaluating the heat flux from the surface temperature. Of particular interest will be the amplitude and phase errors introduced by the algorithms. Such an evaluation will be possible because the actual heat flux is known to be that given by equation (10).

NUMERICAL ALGORITHMS FOR CALCULATING HEAT FLUX FROM SURFACE TEMPERATURE MEASUREMENTS

An alternative to the analog Q-meter is the direct calculation of heat flux from the time dependent surface temperature measured by the gauge. For all but the simplest inputs (and then only if the thermal properties are assumed constant), the solutions to equations (1) and (11) cannot be obtained in closed form, and must be calculated numerically. The particular problem here falls into the general class of inverse heat conduction and ill-posed problems for which there is an extensive literature. (Beck et al. [13] provide an excellent summary of both examples and pitfalls of the various numerical approaches.) This paper will consider two numerical algorithms which have been used for processing thin film gauge data: the first, the finite difference approximation to the exact solution for constant thermal properties proposed by Cooke and Felderman [10], and the second, the simple implicit scheme for variable thermal properties used by Dunn et al. [5]. The focus of the evaluation here will be on the ability of the algorithms to faithfully represent the amplitude and phase of rapidly varying input data, and on their sensitivity to the quantization errors and noise encountered in typical applications.

The Cooke-Felderman Algorithm. This algorithm is based on the integral

solution to equations (1) and (2) for constant thermal properties which is

$$q(0,t) = \left[\frac{\rho Ck}{\pi}\right]^{1/2} \left[\frac{T(0,t)}{\sqrt{t}} + \frac{1}{2}\int_0^t \frac{[T(0,t)-T(0,\lambda)]}{(t-\lambda)^{3/2}}\, d\lambda\right] \qquad (16)$$

The first numerical approximation to equation (16) was proposed by Vidal [1] who used it to calculate heat flux from thin film gauges in shock tunnels. Cooke and Felderman [10] improved Vidal's algorithm by approximating the temperature in equation (16) at time steps Δt with a piece-wise linear signal. The result for the n^{th} realization of the surface heat flux ($t=n\Delta t$) is given by

$$q_n = \left[\frac{\rho Ck}{\pi}\right]^{1/2} 2(\Delta t)^{-1/2} \sum_{i=1}^{n} \frac{T_i - T_{i-1}}{(n-i)^{1/2}+(n-i+1)^{1/2}} \qquad (17)$$

In spite of its obvious advantage over a finite difference solution, equation (17) is valid only if the thermal properties are constant. Moreover, while it has received extensive use in the calculation of heat fluxes in transient environments, the ability of this algorithm to accurately reproduce rapidly varying fluctuations in the unsteady heat flux has not been established.

If the effects of variable thermal properties on the instantaneous heat flux are to be accounted for, there appears to be no alternative to solving the heat conduction equation numerically. (Note, however, that corrections to equation (17) for varying thermal properties have been proposed by Miller [14]). Dunn et al. [4] proposed a technique utilizing a Crank-Nicolson finite difference procedure. Unfortunately, the equations were cast in terms of the similarity variable $\eta = x/\sqrt{\alpha t}$ which rendered the solution incapable of following rapid fluctuations at large time because of the increasing grid spacing. The problem encountered above has been reported in detail in Dunn et al. [5]. However, because of its importance to the problem of resolving fluctuating heat transfer rates, it will be briefly summarized here.

When the heat transfer rate contains a part that fluctuates at frequency ω *, a second scale enters the problem, namely $\sqrt{\alpha/\omega}$, which is properly called the skin depth and is independent of time. The classical solution of a sinusoidal surface-temperature variation (Carslaw and Jaeger, [15]) contains an early-time transient plus the solution:

$$\Delta T(x,t) = A \exp\{-x\sqrt{\omega/\alpha x}\} \cos\{\omega t - x\sqrt{\omega/\alpha}\} \tag{18}$$

Thus the high-frequency portion of the surface-temperature rise has a very shallow penetration, and care must be taken in the numerical work to resolve this thin layer properly. Solutions of equation (1) which use a fixed step size in the η–direction will have a small value of Δx at early time, and a large one at late time. Clearly the solution is to avoid the problem by differencing in x, not η.

Dunn et al. [5] proposed a simple-implicit algorithm given by

$$\frac{\phi(i,j+1)-\phi(i,j)}{t_{j+1}-t_j} =$$

$$\alpha(x_j,t_j)\ \frac{\phi(i+1,j+1)-2\phi(i,j+1)+\phi(i-1,j+1)}{(\Delta x)^2} \tag{19}$$

where ϕ is defined by the Kirchoff transformation (v. Carslaw and Jaeger [15]) by

$$\phi = \int_{T_{ref}}^{T} \frac{k}{k_{ref}}\, dT \tag{20}$$

This equation was solved on a grid of variable size: At every time step, the boundary condition of zero temperature rise was enforced at a depth of $7\sqrt{\alpha_{ref}t}$. The heat transfer rate was found from a second-order accurate expression for the derivative at the surface.

---

*The radial frequency $\omega=2\pi f$ has been used here for convenience.

gauges can be used for the measurement of periodic or statistically stationary heat flux measurement.* The first of these is when the average heat flux is identically zero, in which case the transient part of the solution given by equation (15) dies off and only the periodic component remains. Then equation (3) can be applied directly to the unsteady part of the temperature signal to obtain spectra of the heat flux. This presumes, of course, that the lowest frequencies of interest are above the low frequency cut-off described above and that the thermal properties are nearly constant. The second situation arises when the transient part of the temperature signal contributes only below the cut-off frequency, so that the unsteady part of the signal is uncontaminated by it. In this case, the average heat transfer cannot be determined, but equation (3) can still be shown to be valid for the unsteady heat flux determination.

ACKNOWLEDGEMENTS

The research reported in this paper was supported by the National Aeronautics and Space Administration, Lewis Research Center, Cleveland, Ohio, under grant numbers NAG 3-469 and NAG 3-581. The work was a part of the CUBRC Gas Turbine Research Program under the direction of Dr. Michael Dunn, to whom the authors are indebted for his encouragement and technical insights. The contributions of Paul Seymour and James Sonnenmeier are also gratefully acknowledged.

An earlier version of this paper was presented at the 1987 ASME - JSME Thermal Engineering Joint Conference and published in the proceedings thereof (George et al. [17]).

*The authors are grateful to P. Magari and Professor J. LaGraff of Syracuse University for pointing this out to us.

NOMENCLATURE

A_o	D.C. part of unsteady heat flux signal [W/m^2]
A_1	coefficient in Eq. (10) [W/m^2]
B_1	coefficient in Eq. (10) [W/m^2]
C	thermal capacity [J/(kg K)]
C(u)	Fresnel integral, see Eq. (13)
d	film thickness [m]
ℓ	smallest lateral dimension of film, or depth of substrate [m]
k	thermal conductivity [w/(m)]
S(u)	Fresnel integral, see Eq.(14)
T	temperature of gauge [K]
$\hat{T}$	Fourier transform of T [K-s]
t	time [sec]
x	coordinate in substrate (Fig. 1) [m]
$\dot{q}$	heat flux [w/m^2]
q	Fourier transform of $\dot{q}$ [$W-s/m^2$]
f	frequency [Hz]
$\hat{e}_i$	Fourier transform of input voltage [V-s]
$\hat{e}_{oi}$	Fourier transform of ideal output voltage [V-s]
$\hat{e}_o$	Fourier transform of real output voltage [V-s]
H_{ideal}	frequency response function of ideal system
H_{real}	frequency response function of real system
H_{dep}	defined by Eq. (9)
α	thermal diffusivity of substrate [m^2]
α_f	thermal diffusivity of film [m^2]
ϵ	ratio of quantization step to peak-to-peak signal
λ	integration variable (time) [s]
ρ	density of substrate [kg/m^3]
γ	constant - 0.3989, dimensionless
Δt	time between samples Eqs. 17,21 [s]

REFERENCES

1. Vidal, R.J. Model Instrumentation Techniques for Heat Transfer and Force Measurements in a Hypersonic Shock Tunnel, Cornell Aeronautical Laboratory Report M. AD-917-A-1., 1956.

2. Schultz, D.L. and Jones, T.V. Heat Transfer Measurements in Short Duration Hypersonic Facilties, AGARDograph No. 165., 1973.

3. Dunn, M.G. and Holt, J.L. Turbine Stage Heat Flux Measurements, AIAA/ASME 18th Joint Propulsion Conference, Cleveland, OH, June 21-23, Paper No. 82-1289., 1982.

4. Dunn, M.G., Rae, W.J., and Holt, J.L. Measurement and Analysis of Heat-Flux Data in a Turbine Stage: Part I: Description of Experimental Apparatus and Data Analysis, J. Eng. for Power, Vol. 106, pp. 229-240, Jan. 1986.

5. Dunn, M.G., George, W.K., Rae, W.J., Woodward, S.H., Moller, J.C. and Seymour, P.J. Heat Flux Measurements for the Rotor of a Full-Stage Turbine: Part II: Description of Analysis Techniques and Typical Time Resolved Measurements, ASME 31st Int. Gas Turbine Conf., Dusseldorf, W. Germany, 8-12 June, 1986.

6. Doorly, D.J. and Oldfield, M.L.G. Simulation of the Effects of Shock Wave Passing on a Turbine Rotor Blade, ASME Paper No. 85-GT-112, 1985.

7. Skinner, G.T. Analog Network to Convert Surface Temperature to Heat Flux, J. of the Am. Rocket Society, V.30, pp. 569-570, 1960.

8. Meyer, R.F. A Heat Flux Meter for use with Thin Film Surface Thermometers, NRC Canada Aero Rep. LR-279, 1960.

9. Oldfield, M.L.G., Burd, H.J. and Doe, N.G. Design of Wide-Bandwidth Analogue Circuits for Heat Transfer Instrumentation in Transient Tunnels, Heat Transfer in Rotating Machinery, (Proc. of 16th Symp. of Int. Center for Heat and Mass Transfer, Dubrovnik, Sept.) eds. Metzger and Afgan, Hemisphere Pub., N.Y., 1980.

10. Cook, W.J. and Felderman, E.J. Reduction of Data from Thin-Film Heat Transfer Gauges: A Concise Numerical Technique, AIAA Jour., 4, No.3, pp. 561-562, 1966.

11. Cook, W. J. Determination of Heat-transfer Rates From Transient Surface Temperature Measurements, AIAA Jour., 8, 7, pp. 1366-1368, 1970.

12. Abramowitz, M. and Stegun, I.S. Handbook of Mathematical Functions, National Bureau of Standards, Applied Mathematics Series 55, 1964.

13. Beck, J.V., Blackwell, B. and St. Clair, Jr., C.R. Inverse Heat Conduction - III-Posed Problems, Wiley-Interscience Publication, NY, 1985.

14. Miller, C.G. Comparison of Thin-Film Resistance Heat-Transfer Gages With Thin-Skin Transient Calorimeter Gages in Conventional Hypersonic Wind Tunnels, NASA TM 83197, 1981.

15. Carslaw, H.S. and Jaeger, J.C. Conduction of Heat in Solids, 2nd ed. Section 216, Clarendon Press, 1960.

16. Anderson, J., Tannenhill, R. and Pletcher, R. Computational Fluid Mechanics and Heat Transfer, Hemisphere Press. NY, 1985.

17. George, W.K., Rae, W.J., Seymour, P.J., and Sonnemeier, J.R., An Evaluation of Analog and Numerical Techniques for Unsteady Heat Transfer Measurement with Thin Film Gauges in Transient Facilities, Proc. ASME - JSME Engineering Joint Conference, 2, pp. 611-617, 1987.

LIST OF FIGURES

15b Sensitivity of Cook-Felderman algorithm to quantization noise on input (f_s/f_o = 15, ϵ = 0.12).

15c Sensitivity of Cook-Felderman algorithm to quantization noise on input (f_s/f_o = 7.5, ϵ = 0.12).

15d Sensitivity of Cook-Felderman algorithm to quantization noise on input (f_s/f_o = 3.75, ϵ = 0.12).

16a Sensitivity of simple implicit algorithm to quantization noise on input (f_s/f_o = 30, ϵ = 0.12).

16b Sensitivity of simple implicit algorithm to quantization noise on input (f_s/f_o = 15, ϵ = 0.12).

16c Sensitivity of simple implicit algorithm to quantization noise on input (f_s/f_o = 7.5, ϵ = 0.12).

16d Sensitivity of simple implicit algorithm to quantization noise on input (f_s/f_o = 3.75, ϵ = 0.12).

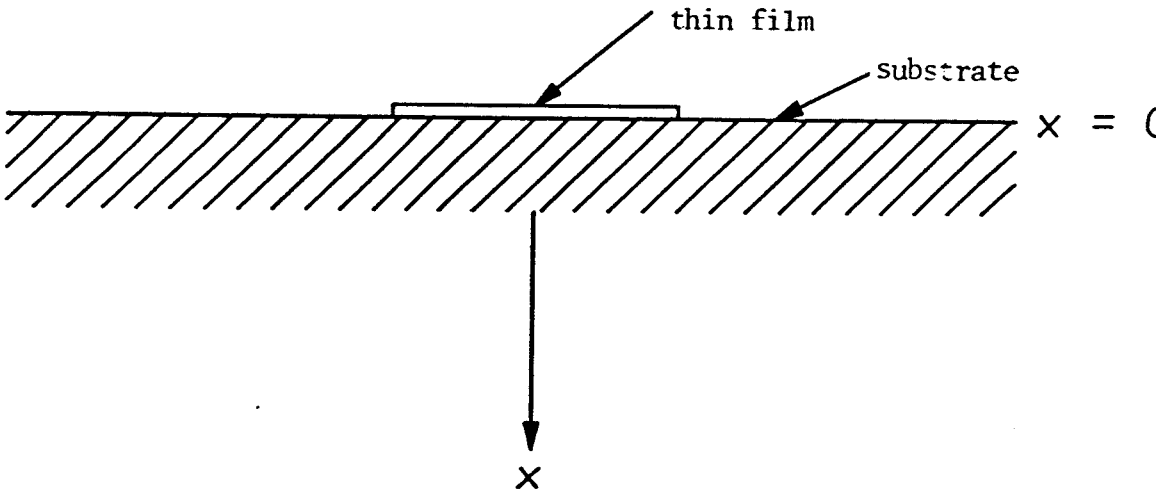

Figure 1. Coordinate system for Equation 1.

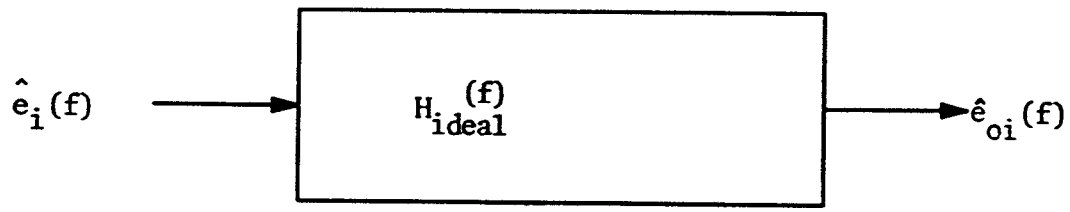

Figure 2a. Schematic of ideal linear system.

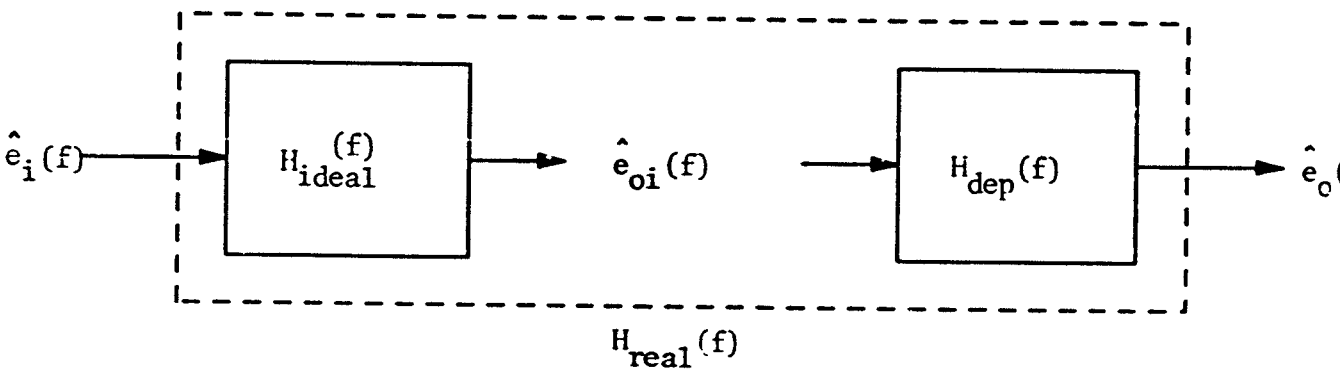

Figure 2b. Schematic of real linear system showing departure from ideal.

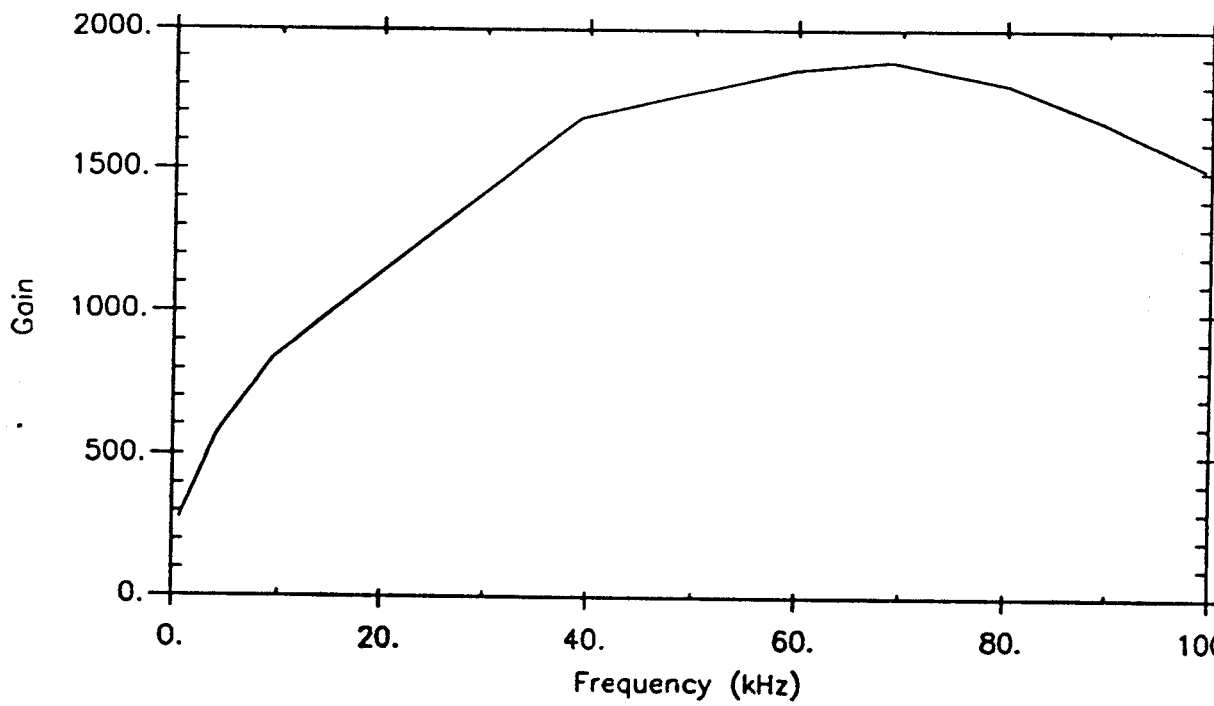

Figure 3a. Gain characteristic for Q-meter (9).

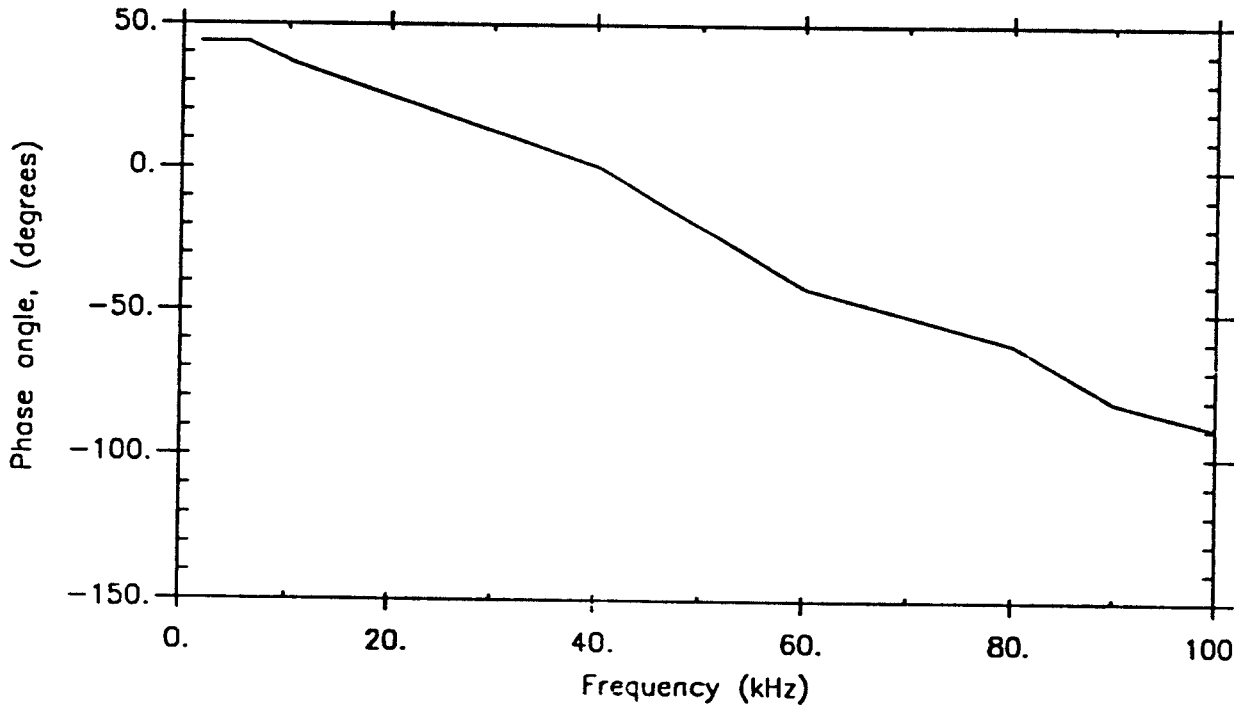

Figure 3b. Phase characteristic for Q-meter (9).

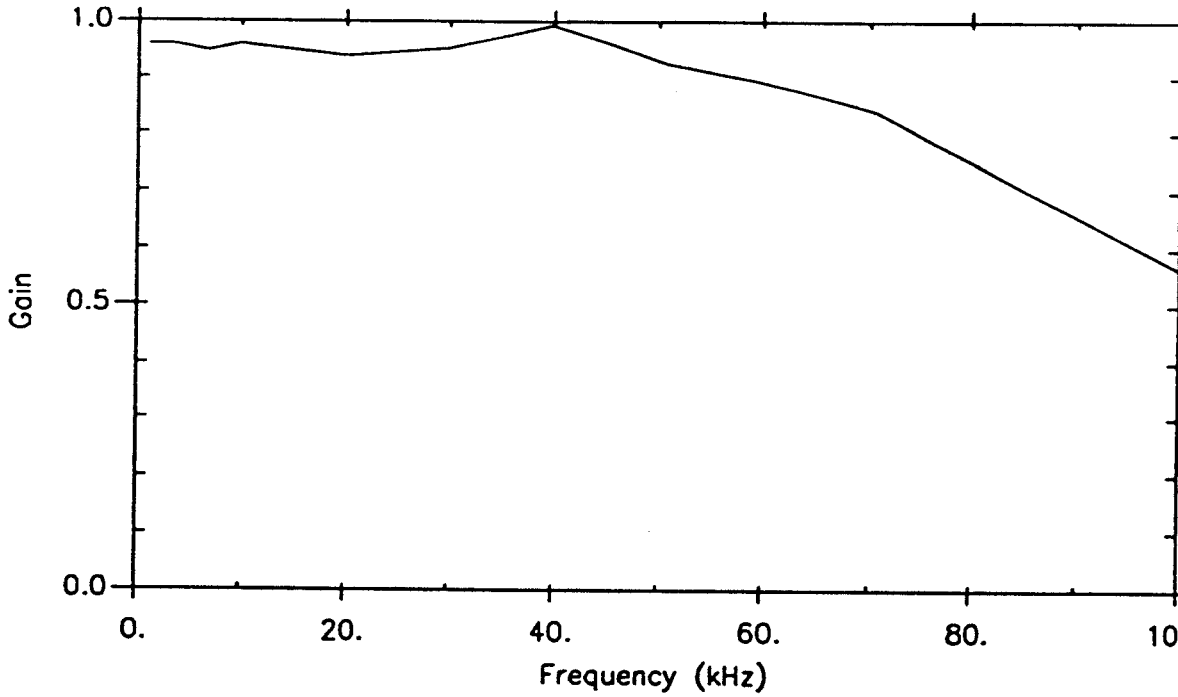

Figure 4a. Gain characteristic for difference from ideal response.

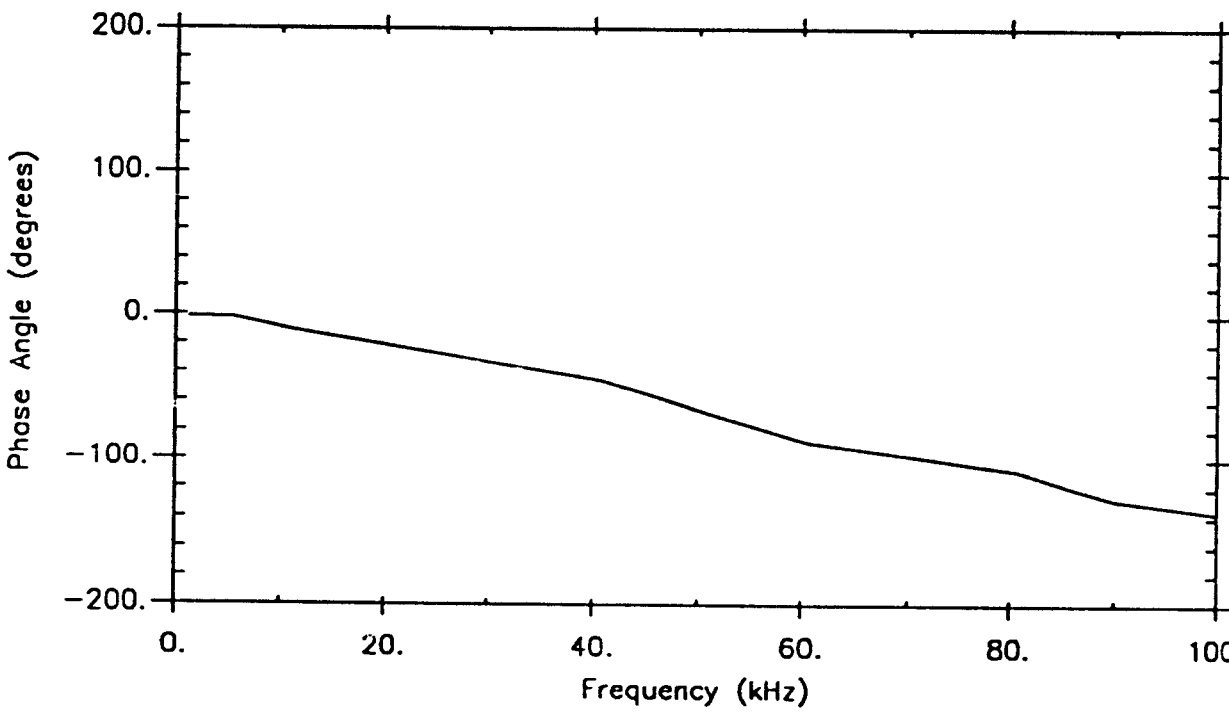

Figure 4b. Phase characteristic for difference from ideal response.

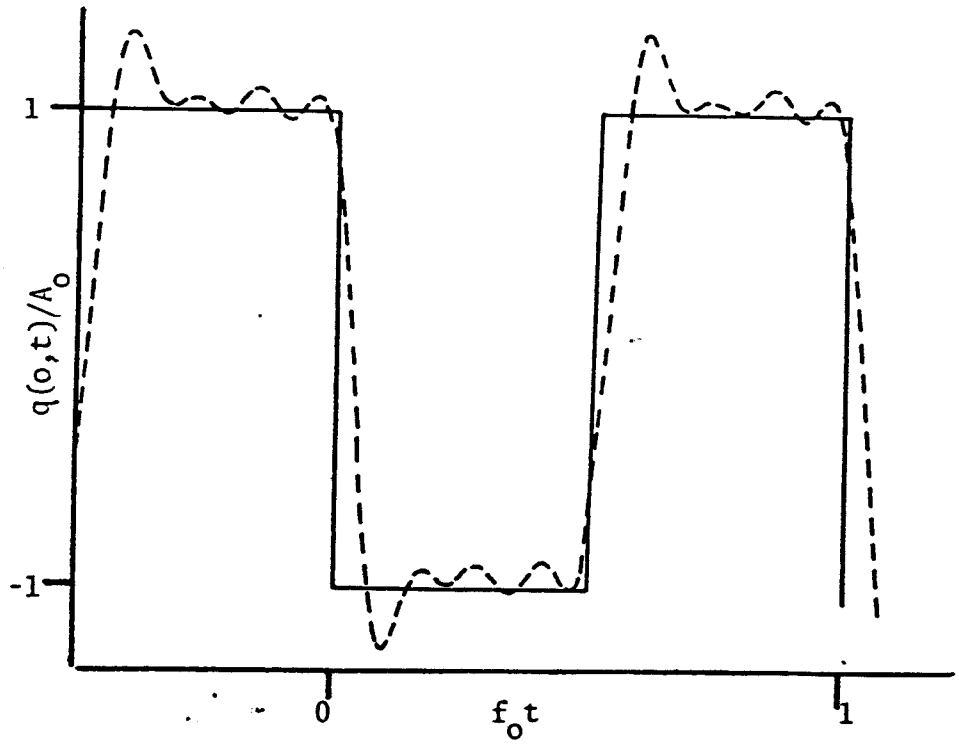

Figure 5. Response of Q-meter to input which would ideally generate a square wave output.

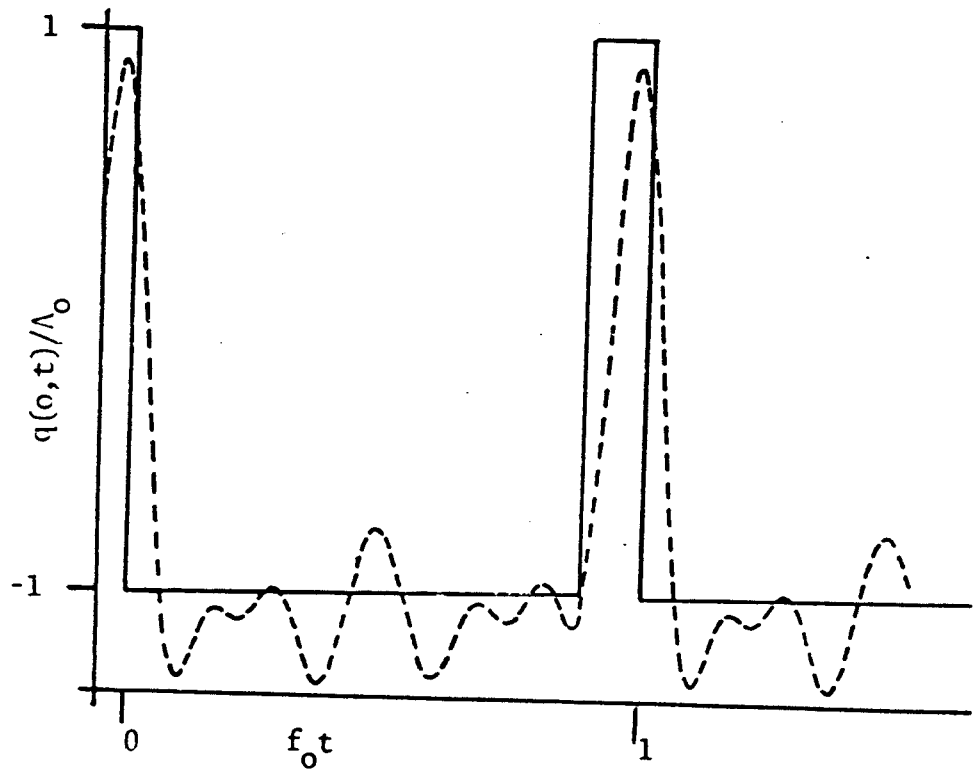

Figure 6. Response of Q-meter to input which ideally generates a pulse train output.

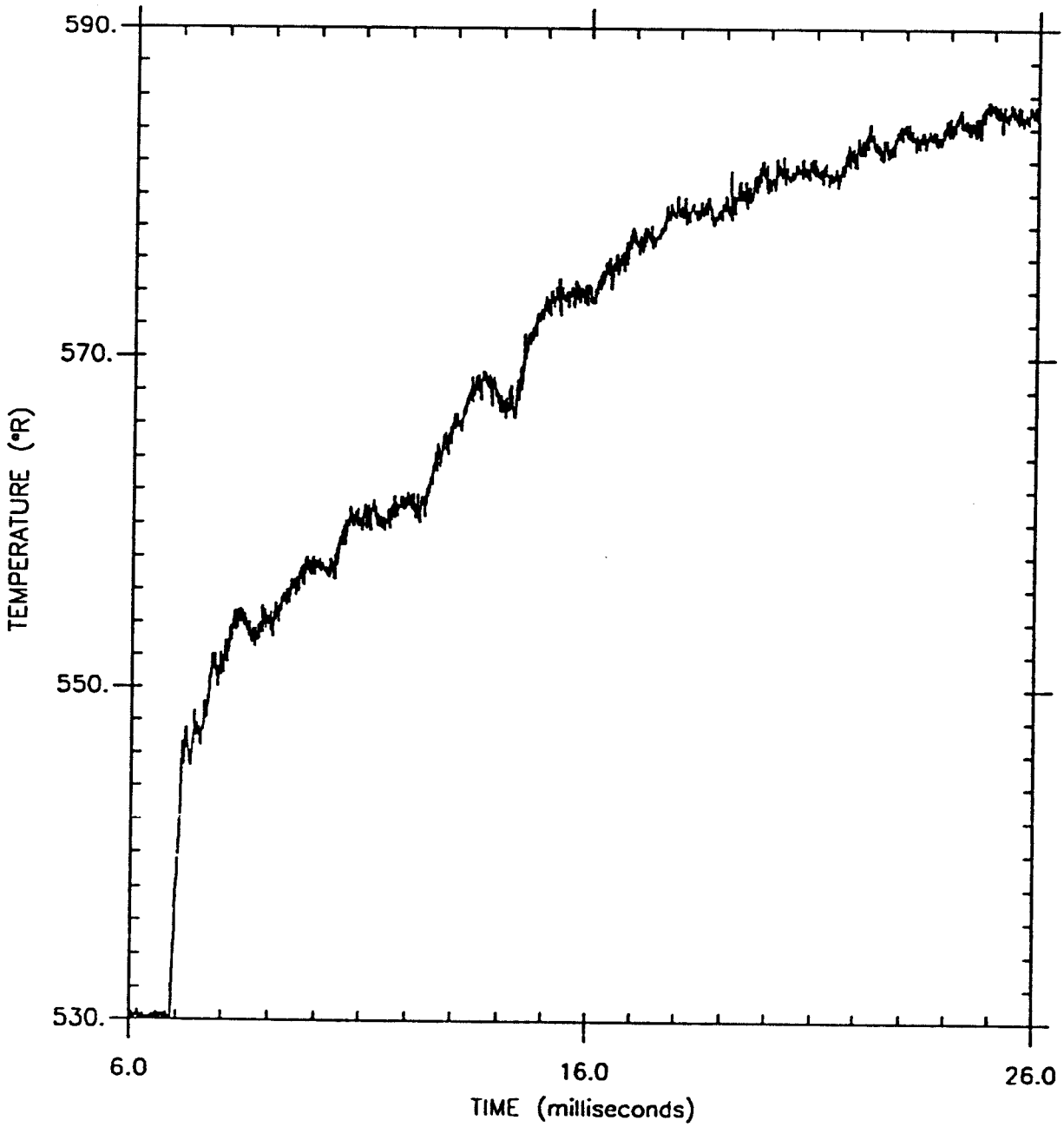

Figure 7. Typical surface temperature measured by this film gauge on turbine rotor in a shock tunnel.

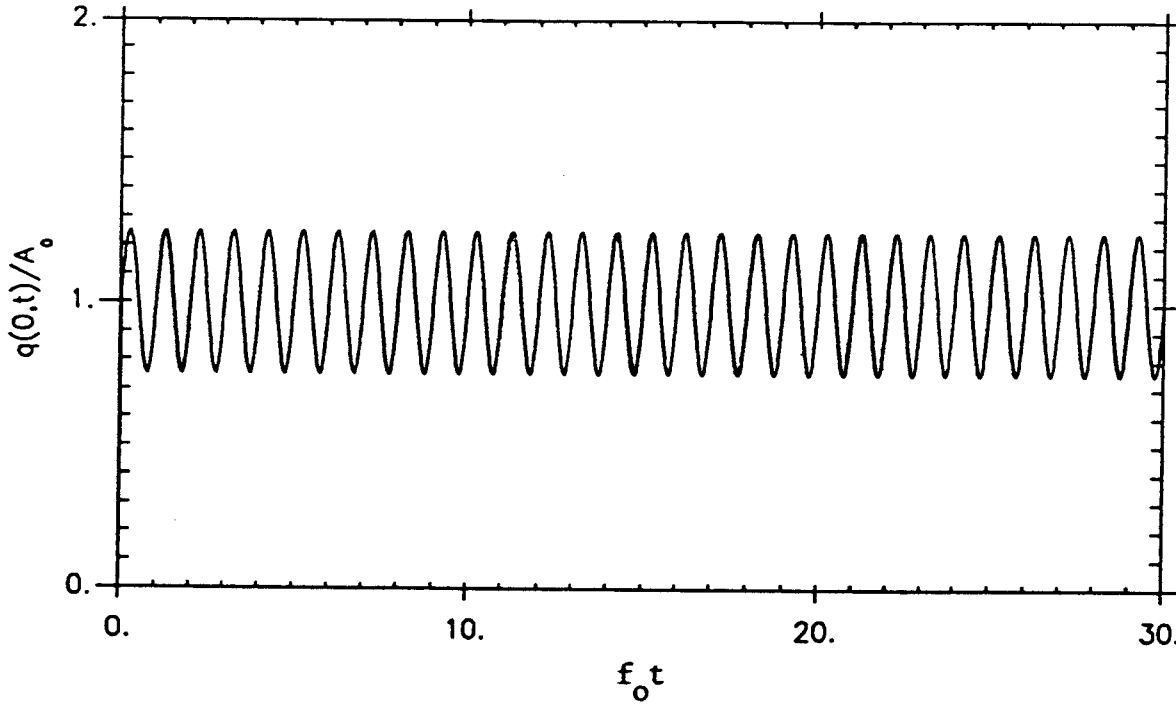

Figure 8a. Step rise in heat flux plus sinusoidal oscillation ($A_1/A_o = 0$, $A_1/A_o = 1/4$ in eqn. 10).

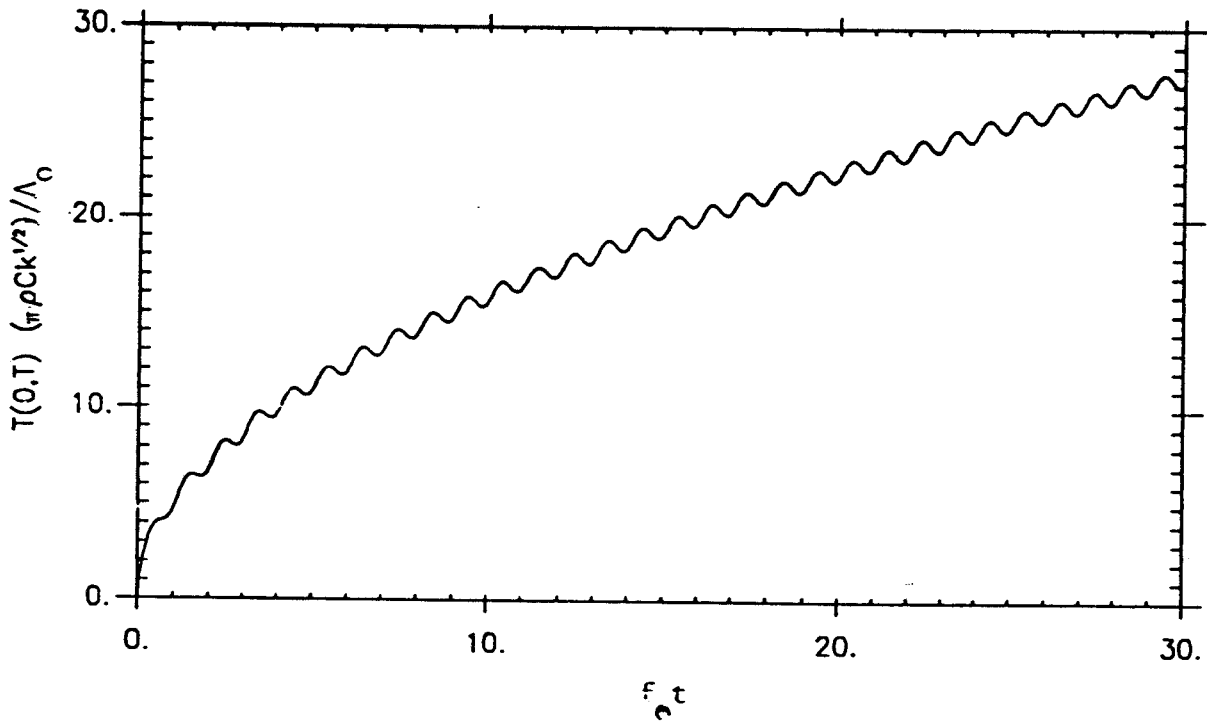

Figure 8b. Response of surface temperature to heat flux in Fig. 8a.

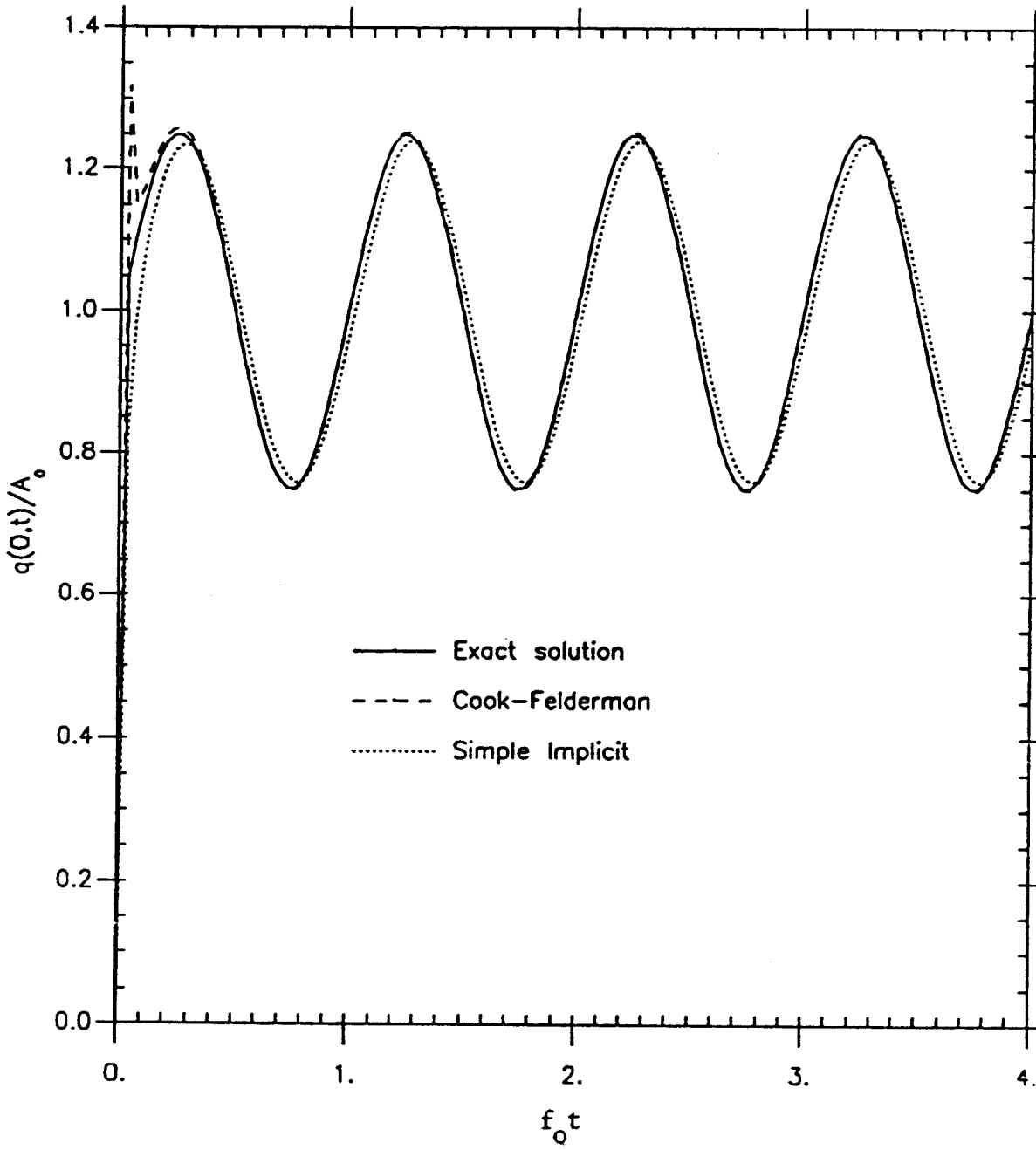

Figure 9. Computed response to Fresnel integral temperature ($f_s/f_o = 30$).

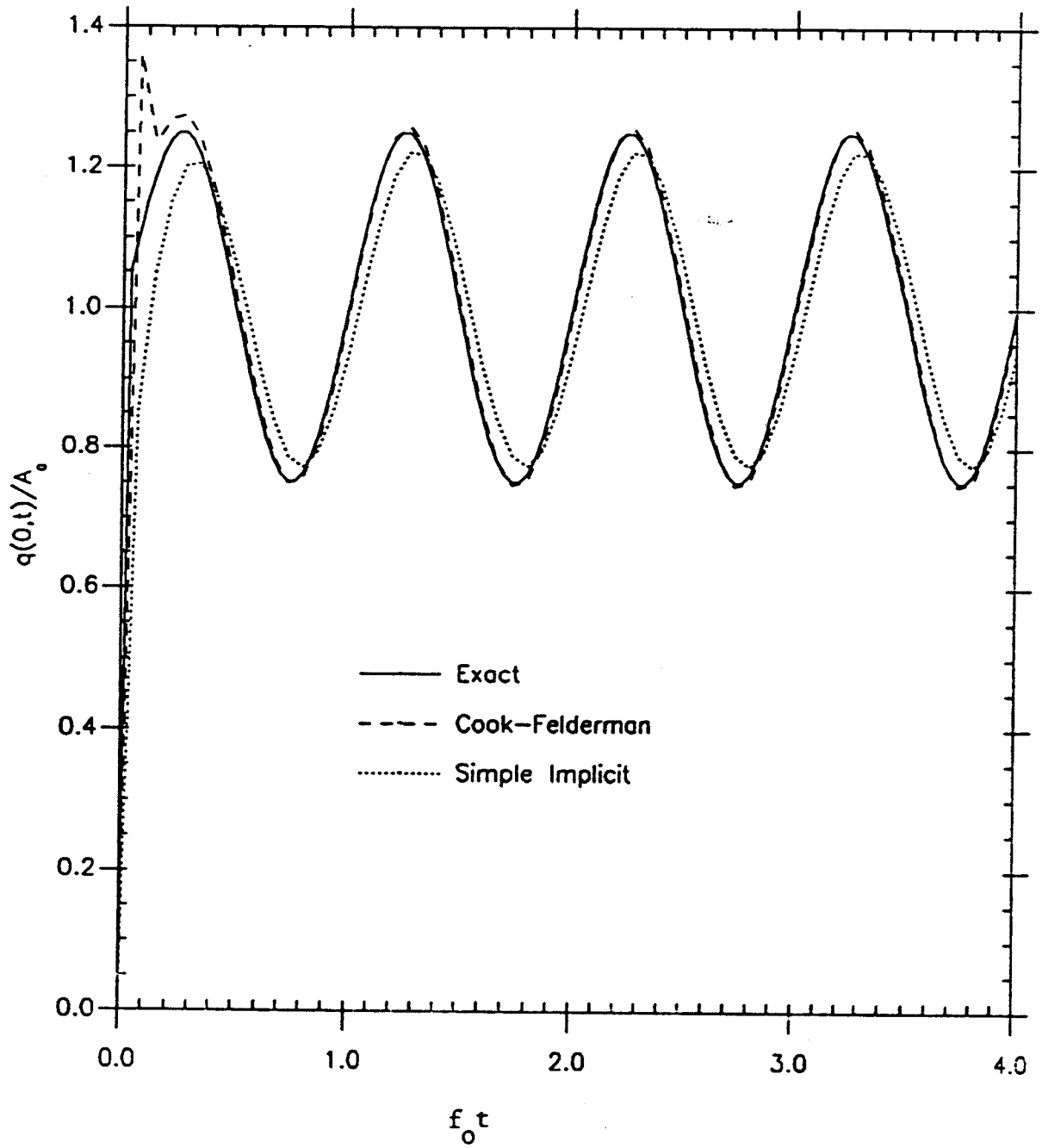

Figure 10. Computed response to Fresnel integral temperature (f_s/f_o = 15).

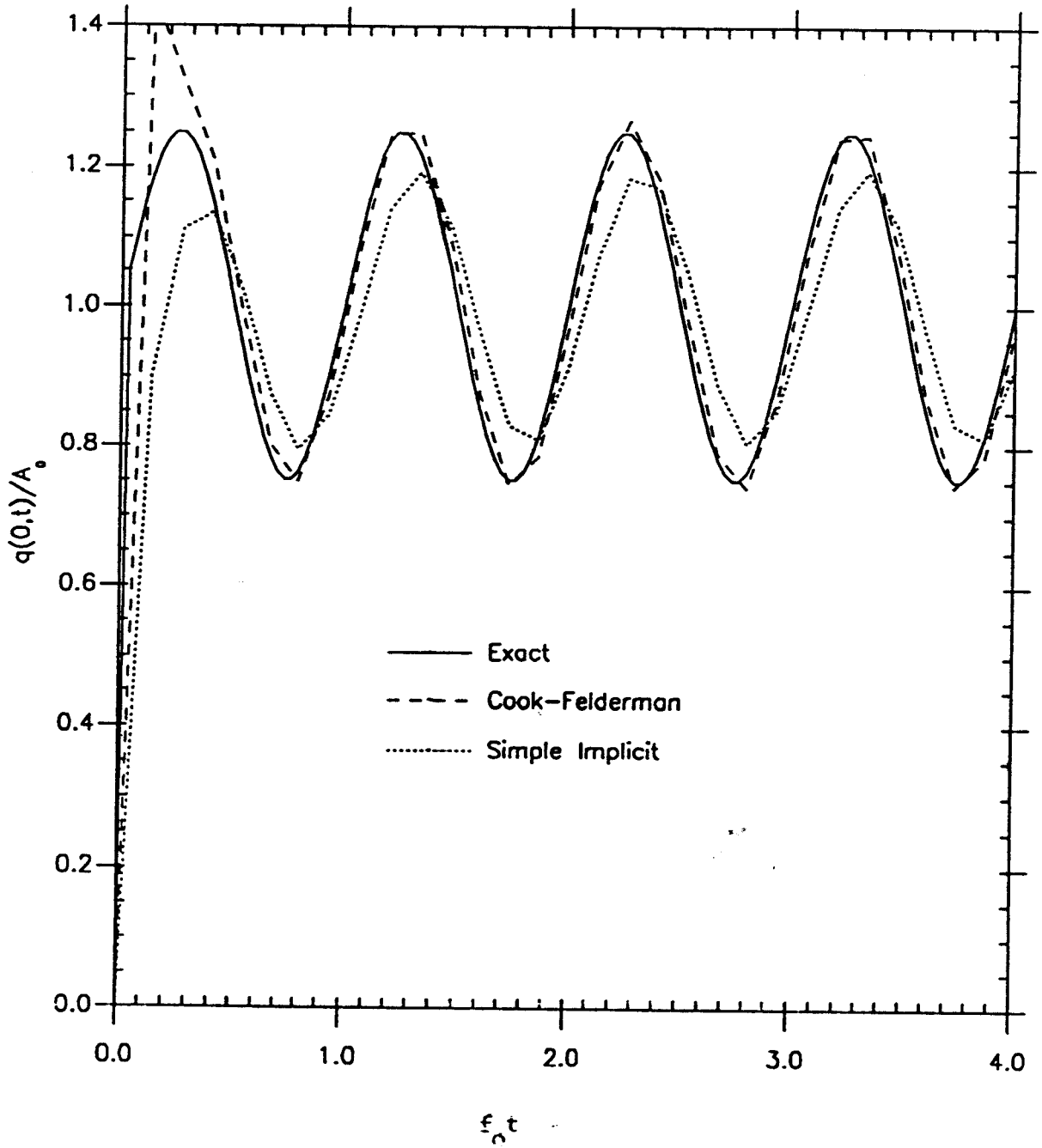

Figure 11. Computed response to Fresnel integral temperature (f_s/f_o = 7.5).

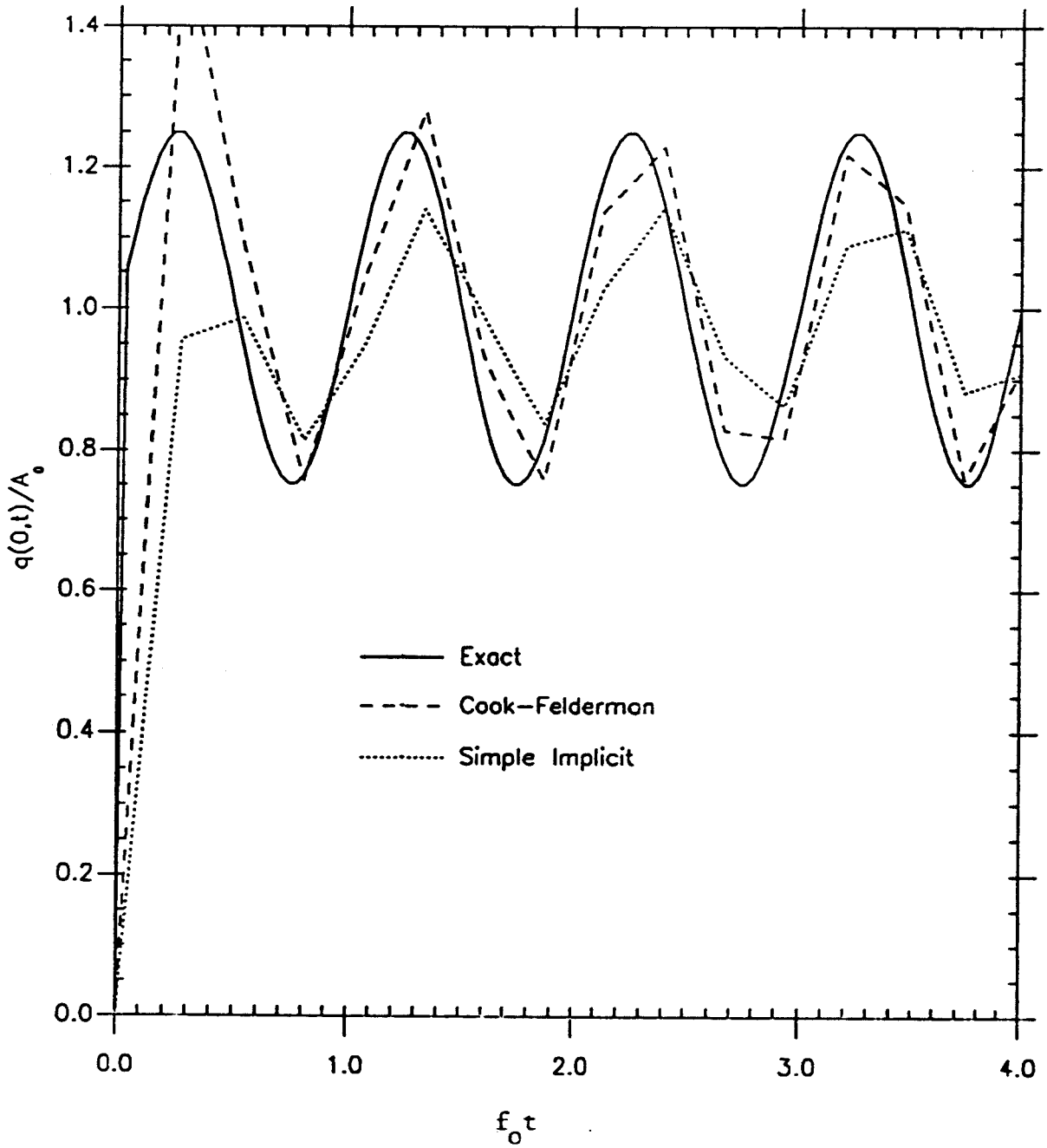

Figure 12. Computed response to Fresnel integral temperature ($f_s/f_o = 3.75$).

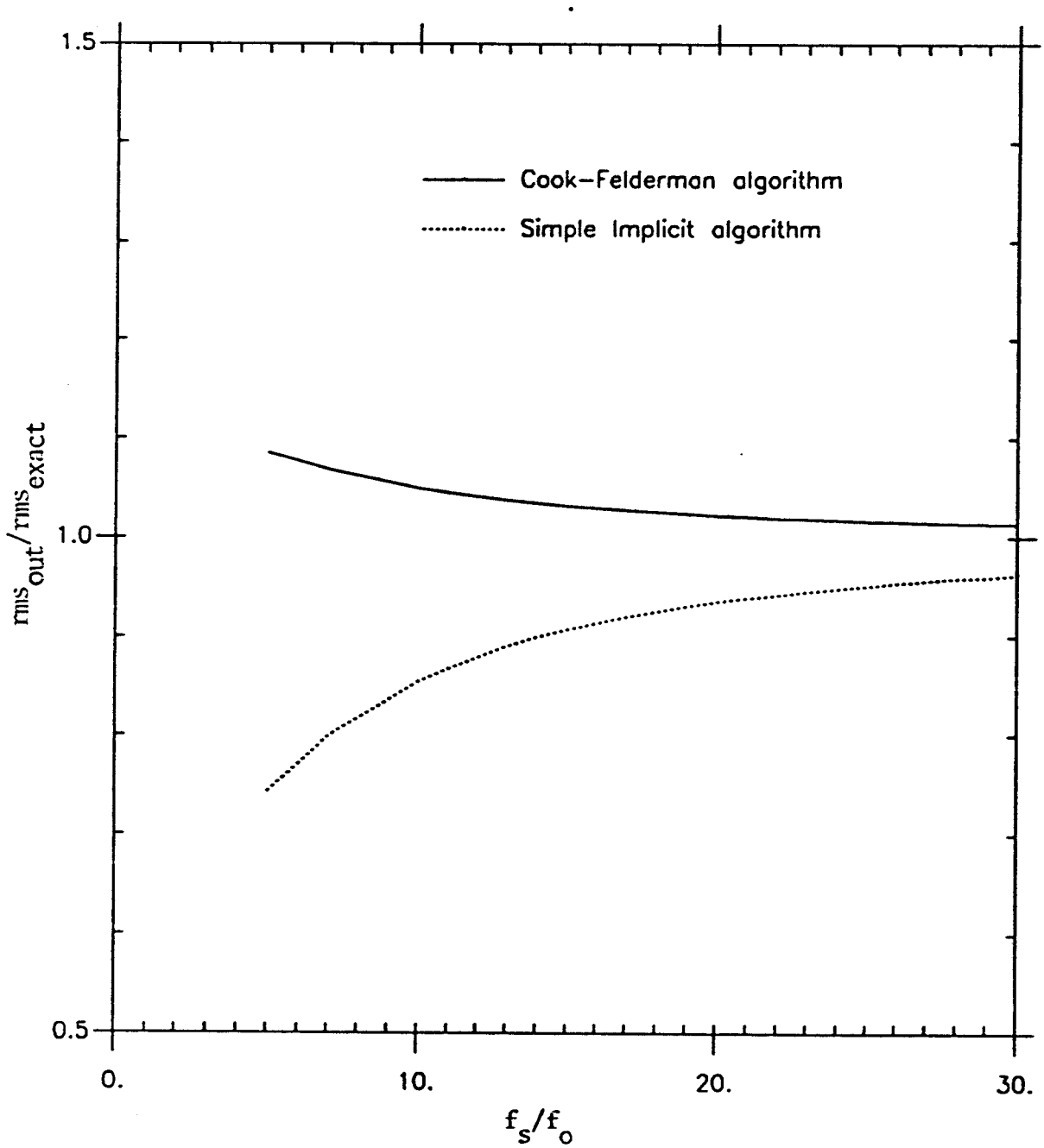

Figure 13. Ratio of computed rms output to rms of exact solution.

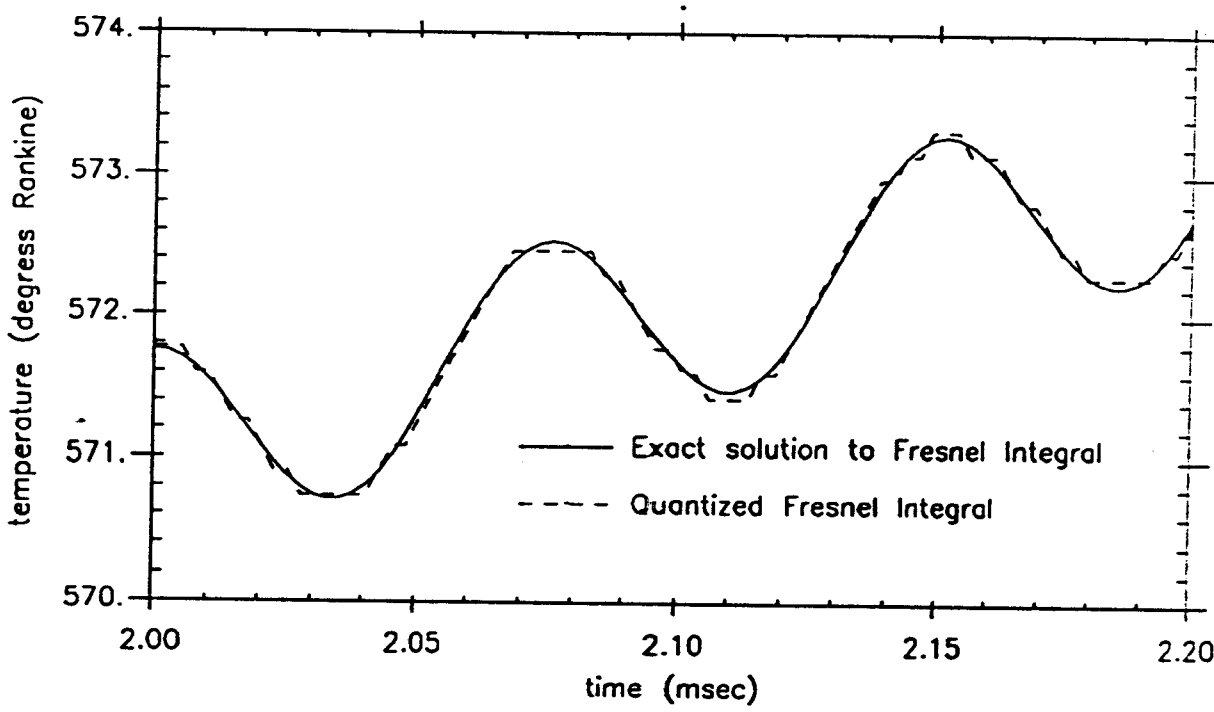

Figure 14a. Typical Fresnel integral temperature input with and without 8 bit quantization.

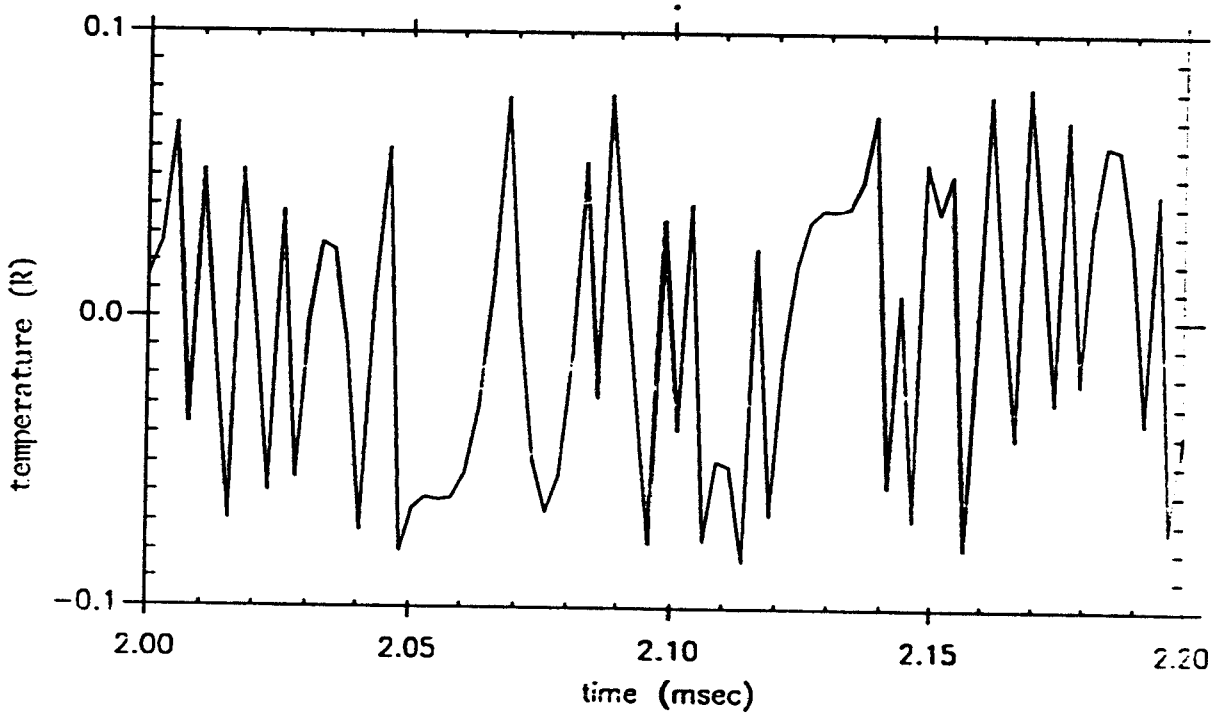

Figure 14b. Difference between exact and quantized Fresnel integral temperatures in Figure 14a.

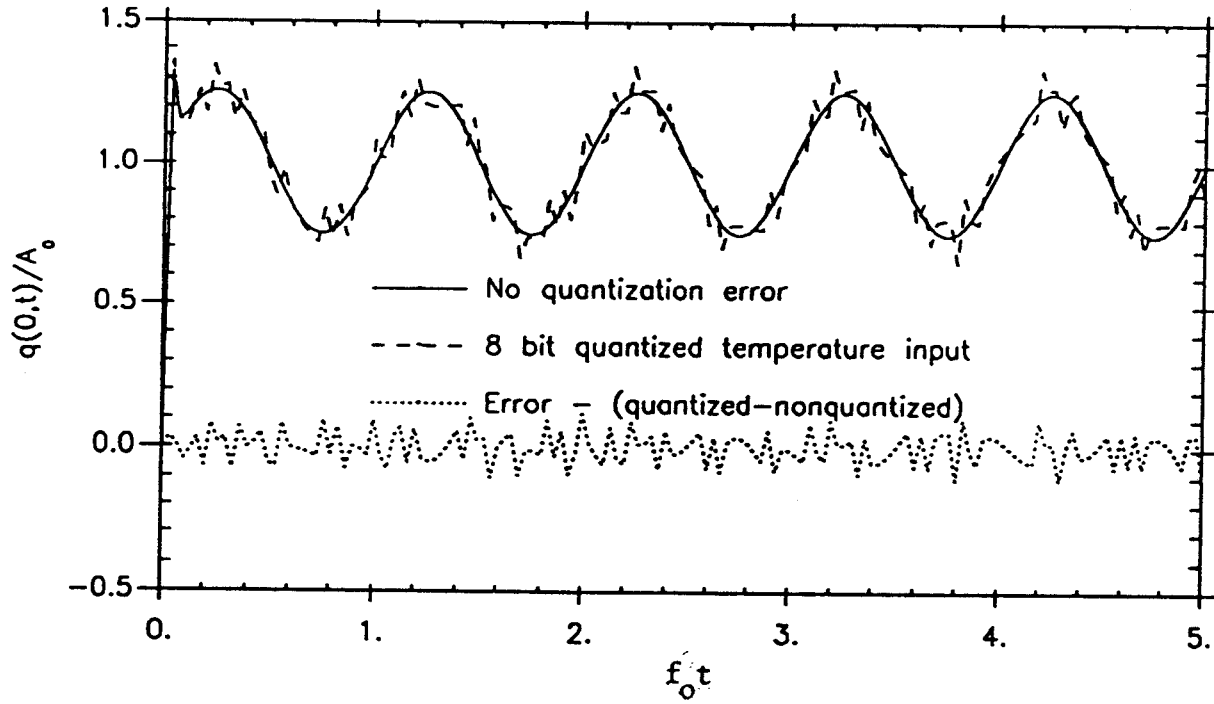

Figure 15a. Sensitivity of Cook-Felderman algorithm to quantization noise on input (f_s/f_o = 30, ϵ = 0.12).

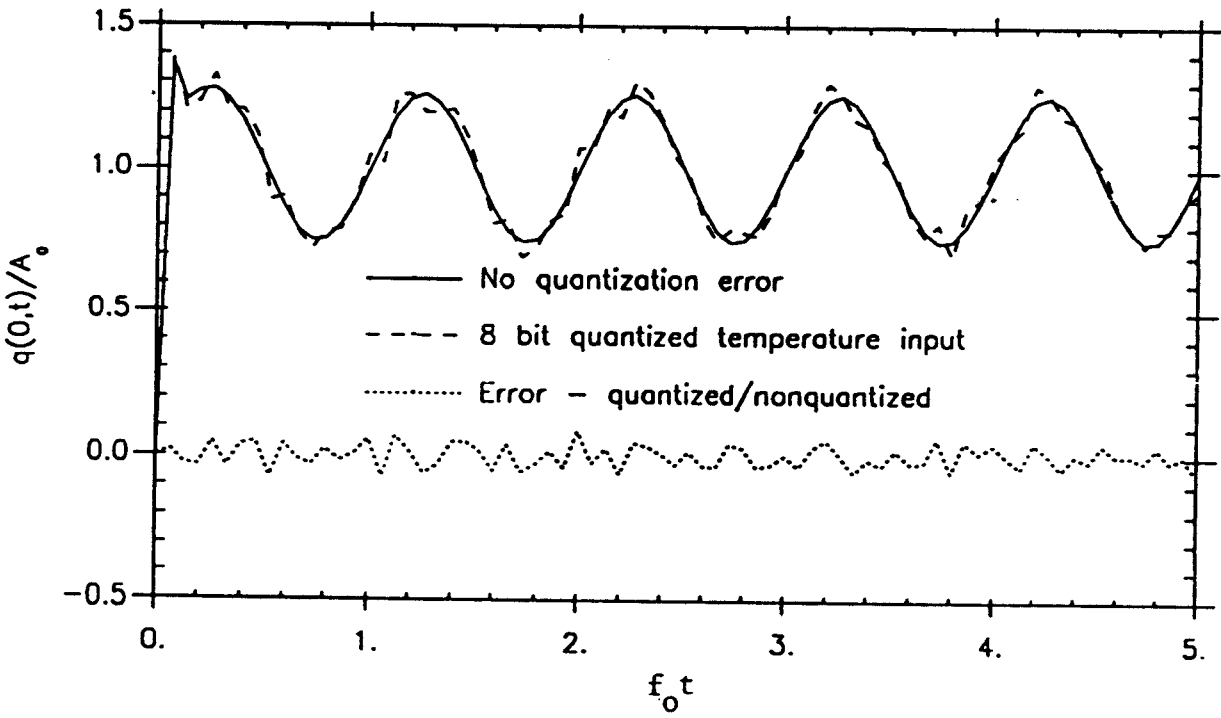

Figure 15b. Sensitivity of Cook-Felderman algorithm to quantization noise on input (f_s/f_o = 15, ϵ = 0.12).

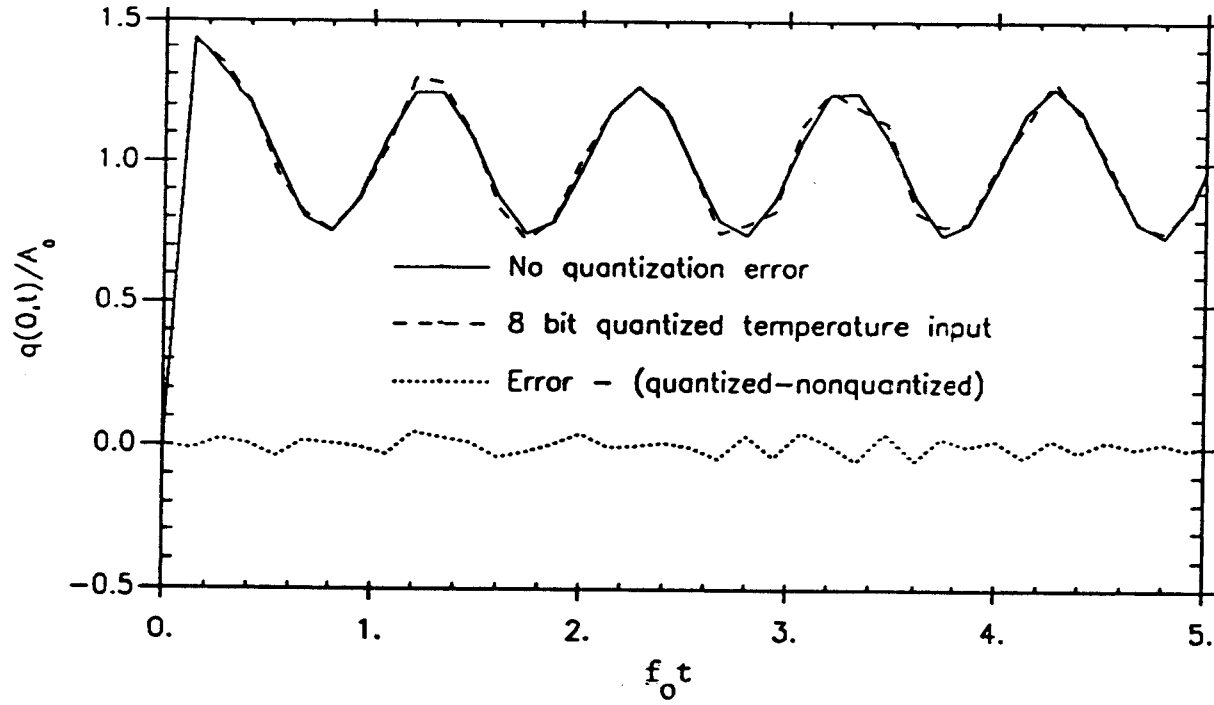

Figure 15c. Sensitivity of Cook-Felderman algorithm to quantization noise on input (f_s/f_o = 7.5, ε = 0.12).

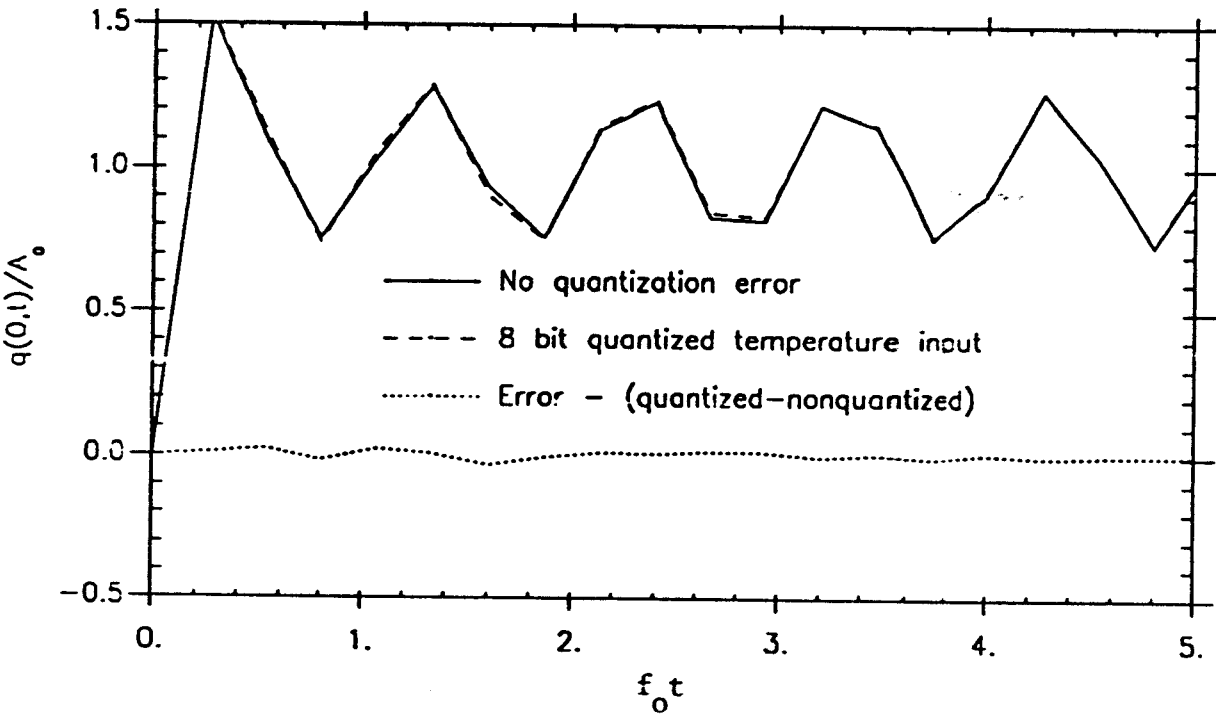

Figure 15d. Sensitivity of Cook-Felderman algorithm to quantization noise on input (f_s/f_o = 3.75, ε = 0.12).

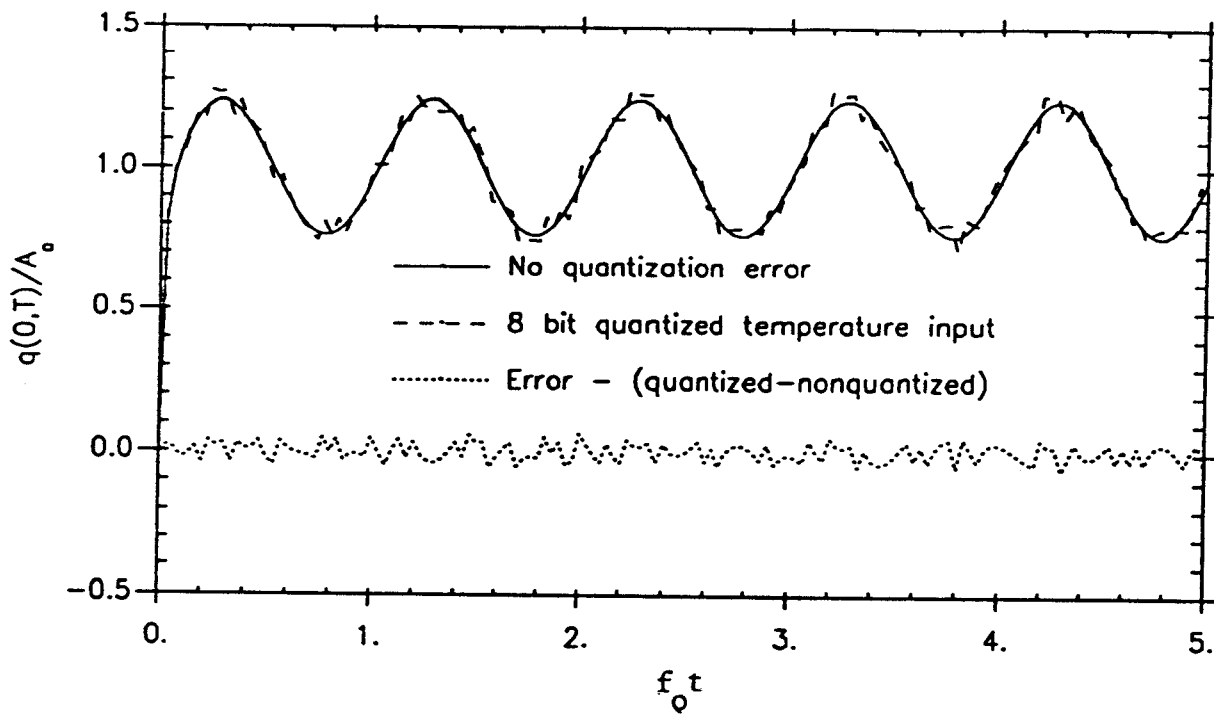

Figure 16a. Sensitivity of simple implicit algorithm to quantization noise on input (f_s/f_o = 30, ε = 0.12).

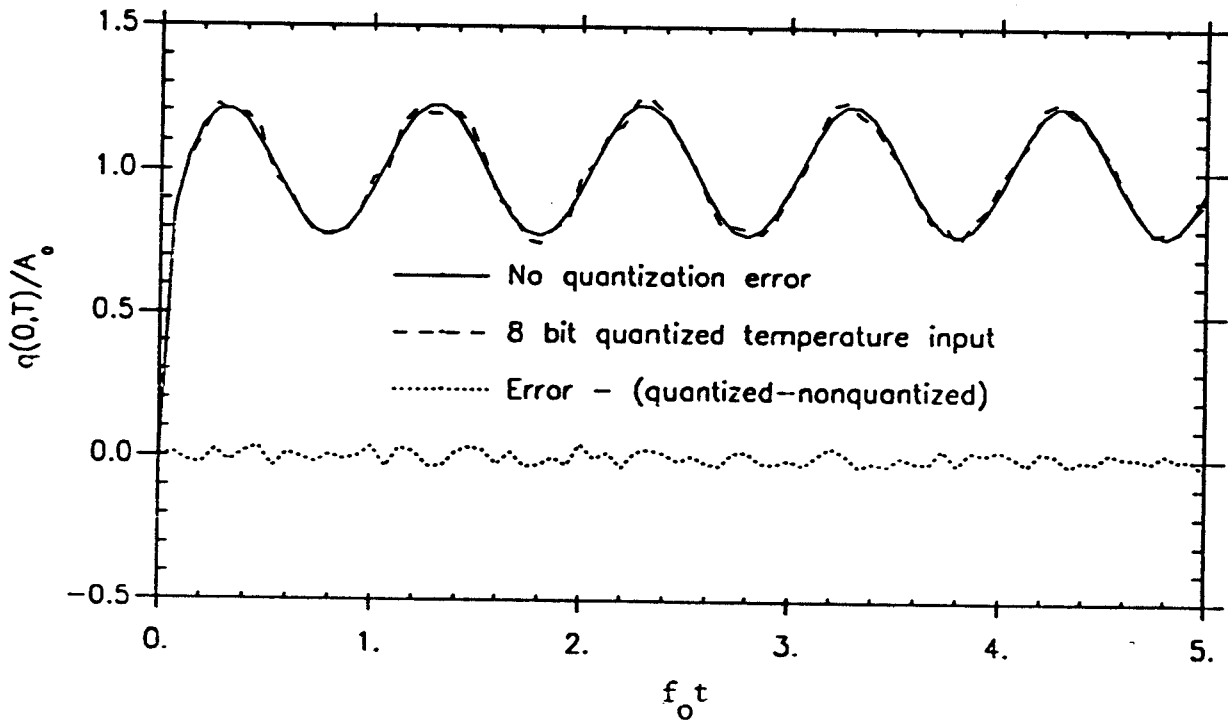

Figure 16b. Sensitivity of simple implicit algorithm to quantization noise on input (f_s/f_o = 15, ε = 0.12).

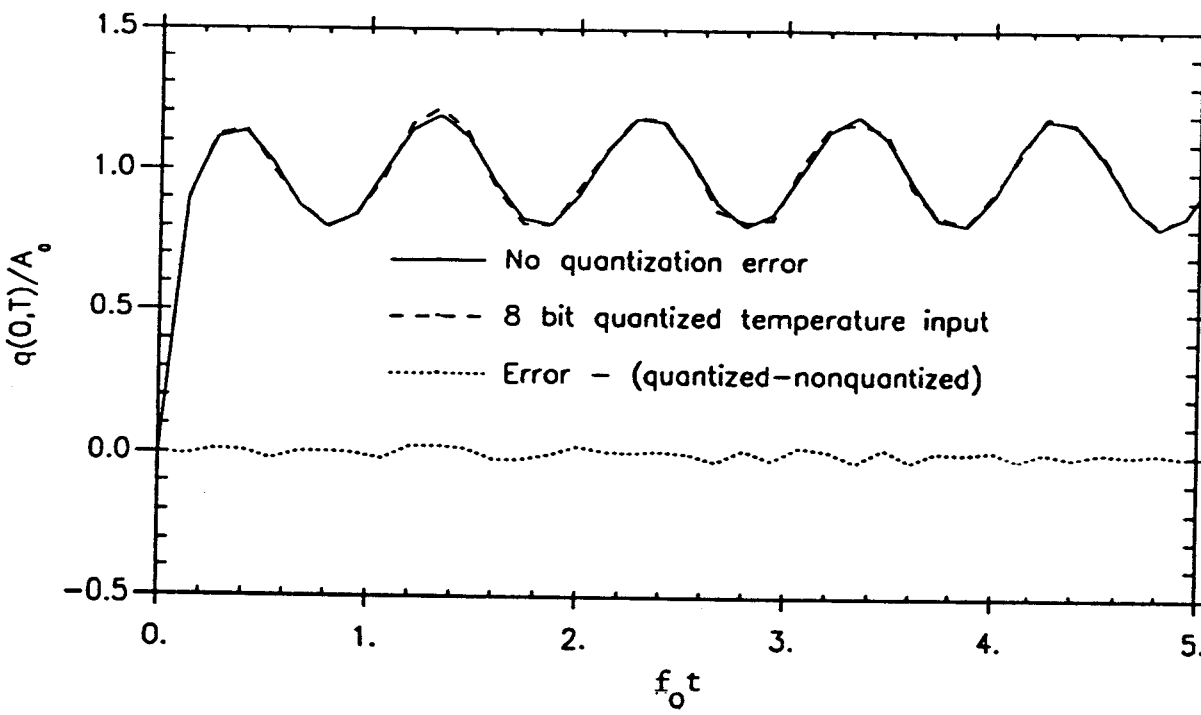

Figure 16c. Sensitivity of simple implicit algorithm to quantization noise on input (f_s/f_o = 7.5, ε = 0.12).

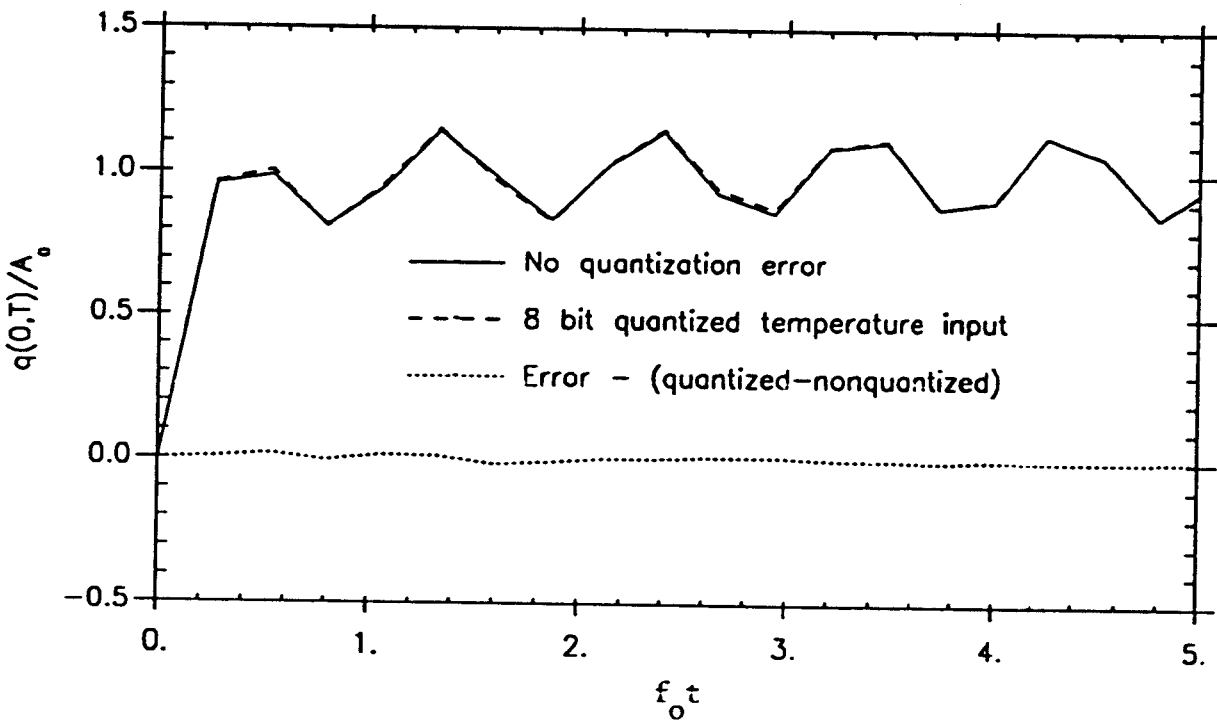

Figure 16d. Sensitivity of simple implicit algorithm to quantization noise on input (f_s/f_o = 3.75, ε = 0.12).